Simplified trajectory method for modeling gas–surface scattering: The NO/Pt(111) system

D. C. Jacobs[a] and R. N. Zare
Department of Chemistry, Stanford University, Stanford, California 94305

(Received 19 December 1988; accepted 22 May 1989)

A model is presented to describe the dynamical processes of trapping/desorption as well as direct and indirect inelastic scattering on single-crystal surfaces. Newton's equations of motion are integrated for a system consisting of a rigid rotor interacting with a slab of 19 surface atoms. The surface atom which is closest to the center of mass of the molecule is permitted to translate only along the surface normal. In turn, this mobile surface atom is harmonically coupled to a microcanonical heat bath consisting of three subsurface atoms. This method is much less computationally intensive than the typical generalized Langevin equation (GLE) approach. Direct comparison is made between the predictions of this model and experiment for the NO/Pt(111) system. In the case of trapping/desorption, the model accurately describes the observed dependence of rotational alignment on rotational quantum number. For the inelastic scattering regime, the model successfully reproduces the degree of rotational excitation and qualitatively accounts for the observed rotational alignment. In addition, the model predicts correlations between final state velocity and final state rotational angular momentum (both direction and magnitude), as well as the effect of molecular orientation and surface impact parameter on the overall trapping probability.

I. INTRODUCTION

Over the past several years, an assortment of dynamical models has been proposed to describe the interaction of molecules with solid surfaces.[1–18] Utilizing various approximations of the surface, the molecule, and the surface–molecule potential, these models treated the processes of direct and indirect inelastic scattering, adsorption, desorption, diffusion, dissociation and recombination. The earliest simulations involved only a rigid surface[1–6] or a cubic mass.[7–10] However, more sophisticated classical trajectory treatments now include surface motion by approximating the surface as a simple harmonic oscillator,[5] a chain of harmonic oscillators,[11,12] or a slab of mobile surface atoms coupled to a heat bath [generalized Langevin equation (GLE) approach].[5,13–18]

The goal of a practical model is to provide an adequate description of the observed physical phenomena with a minimal amount of computation. The compromise between these two aspects is determined by the number and severity of approximations used to represent the gas–surface dynamics. The processes of trapping/desorption and direct and indirect inelastic scattering require both the inclusion of thermal surface motion as well as the use of a realistic surface–molecule potential.

We have constructed a relatively simple stochastic trajectory model that combines the realistic surface potential of a two-dimensional slab (as used in a GLE approach) with limited surface motion (as approximated by a one-dimensional harmonic chain model). Our simulations have clear advantages over the simple cubic models which treat the surface as a flat plane or those models which use a rigid two-dimensional surface.

Our approach incorporates surface motion only in the direction of the surface normal. This approximation is based on the principle that surface phonon motion is dominated by out-of-plane displacements of the surface atoms[19] and that translational-to-surface momentum transfer occurs primarily in the direction of the surface normal. Indeed, experiments which have examined the inelastic scattering of He and Ne from surfaces have been sensitive to only those phonon modes that include appreciable motion along the surface normal.[20] Furthermore, the transfer of normal to tangential momentum is primarily mediated through surface corrugation and not lateral motion of the surface atoms. Additionally, the net force exerted on the molecule by the surface, is most sensitive to the instantaneous out-of-plane position of the nearest surface atom. The relative positions of the other surface atoms, certainly affect the overall force. However, energy transfer is dominated by the short-range repulsive part of the potential. Therefore, we simplify our description of the surface motion by permitting only the surface atom closest to the NO molecule to translate, and then only in the direction of the surface normal.

This mobile surface atom couples to a microcanonical heat bath, represented by three mobile subsurface atoms. Because the time scale of single or multiple collisions (0.2–2 ps) is comparable with a surface vibrational period ($\sim$1 ps), the thermal bath need not be large. We use three subsurface "ghost" atoms, harmonically coupled in a linear chain,[11–13] to simulate energy exchange between the mobile surface atom and the bulk crystal. The empirical surface–molecule potential, adapted from the work of Muhlhausen, Williams, and Tully,[18] consists of a sum of pairwise–additive interactions between the NO molecule and each of nineteen surface atoms in the slab. Individual stochastic trajectories for this system are numerically integrated on a VAX computer.

Direct and indirect inelastic scattering are simulated in

[a] Current address: Department of Chemistry, University of Notre Dame, Notre Dame, IN 46556.

 0021-9606/89/173196-12$02.10

the usual manner. Initial conditions for each trajectory are randomly chosen from a distribution, characterized by the experimental conditions reported by Jacobs *et al.*[21] Those trajectories which approach the surface once and then retreat are considered "direct," more than once are called "indirect," and those that do not escape within the integration period are termed "trapped."[5] Instead of trying to simulate desorption, which requires very large integration times, we utilize microscopic reversibility[22,23] to deduce information about the desorption dynamics from simulations of the adsorption process.

Recently, Jacobs *et al.*[24] have measured the rotational alignment distributions of NO($v = 0$) subsequent to its desorption from Pt(111). Their results indicate that molecules desorbing with a large amount of rotation ($J > 15$) preferentially rotate in the plane of the surface. In a separate study,[21] they measured the rotational population and alignment distributions for the NO/Pt(111) system in the regime of direct and indirect inelastic scattering. They observed a significant amount of energy transfer from both the initial beam energy and surface vibration into nuclear rotation of the scattered molecules. The corresponding rotational alignment data showed a strong preference for the scattered molecule to rotate in a plane normal to the surface. These intriguing experimental observations stimulated interest in the development of classical trajectory simulations that could be run on a minicompter, such as a VAX, rather than on a supercomputer. The proposed model not only emulates the experimental data but it succeeds in revealing additional details about the mechanisms of inelastic scattering, trapping and desorption.

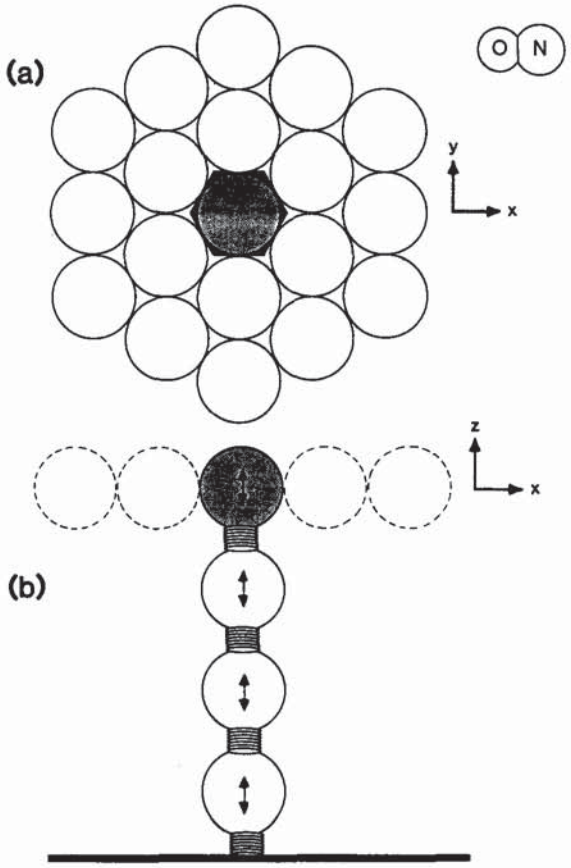

FIG. 1. Schematic of Pt(111) slab. (a) Surface planar and (b) cross-sectional views of the slab show the 18 static surface atoms, the one mobile surface atom and the three mobile subsurface atoms. The hexagonal shaded area defines the active zone which is defined relative to the position of the NO molecule (drawn to scale).

II. THEORY

The fcc(111) substrate is represented by a slab containing nineteen surface atoms (eighteen stationary atoms and one "active" atom) with three subsurface atoms located directly below the active surface atom (Fig. 1). The one active surface atom and the three subsurface atoms are allowed to translate only in the direction normal to the surface. The four mobile atoms are coupled to each other through a linear harmonic chain. The chain is terminated by a connection to a stationary substrate block. The four spring constants are chosen to be identical and have been selected to yield a realistic surface phonon frequency,[17,25] on the order of 10^{12} Hz. The equilibrium positions of the nineteen surface atoms are fixed according to the known structure of the Pt(111) surface. The equilibrium positions of the three subsurface ghost[17] atoms need not be specified within the equations of motion. It should be noted that the three subsurface atoms are not meant to represent those found in the real surface. Instead, they merely simulate a thermal bath to which the mobile surface atom is coupled.

The active surface atom is defined to be that which is closest to the center of mass of the molecule at any given instant in time. When the molecule leaves its current "active zone" (as indicated by the shaded area in Fig. 1), the model switches the substrate such that the molecule finds itself entering a new active zone, surrounded again by eighteen stationary surface atoms.[26] Throughout the entire trajectory, the active zone tracks the molecule. The relative positions and velocities of the mobile solid atoms are preserved during a switch of active zones. This simplification simulates the fact that surface motion is coupled in the X–Y plane, and

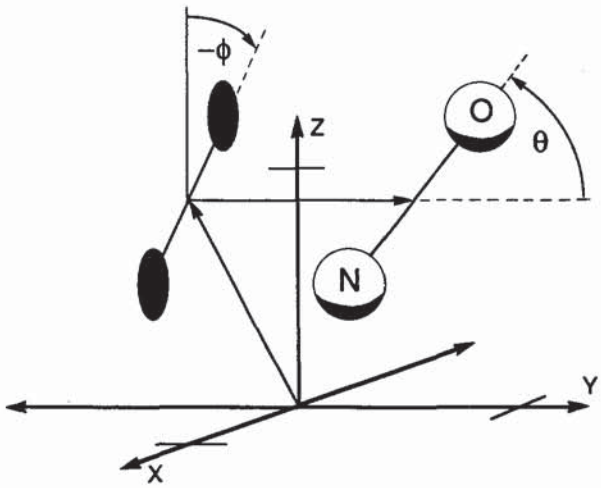

FIG. 2. Molecular coordinate system. The center of mass is specified in Cartesian coordinates while the molecular orientation is defined with respect to the angles θ and ϕ.

therefore neighboring surface atoms will assume similar extensions in the Z direction at a given instant in time.

The molecule is represented by a rigid rotor. The exclusion of vibrational motion not only permits larger integration time steps, i.e., shorter computation time, but it also eliminates the problem associated with constraining the trajectory to be characteristic of the molecule in a particular vibrational quantum state. The rigid rotor approximation appears valid, in that zero-point vibration is much faster than the timescale of the collision, and vibrational excitation in nonreactive scattering has been shown to be quite small for NO/Pt(111).[18,27] Despite the classical treatment of rotational motion, both initial and final rotational states are binned into rotational quantum levels, N. The populations in the rotational bins are divided by $(2N+1)$ in order to correct for the scaling of bin widths with rotational energy.

The system can be completely described by nine equations of motion:

$$\frac{d^2}{dt^2} z_{s1} = \omega^2 (z_{s2} - 2z_{s1}), \tag{1a}$$

$$\frac{d^2}{dt^2} z_{s2} = \omega^2 (z_{s3} - 2z_{s2} + z_{s1}), \tag{1b}$$

$$\frac{d^2}{dt^2} z_{s3} = \omega^2 (z_{s4} - 2z_{s3} + z_{s2}), \tag{1c}$$

$$\frac{d^2}{dt^2} z_{s4} = \omega^2 (z_{s3} - z_{s4}) - \frac{1}{M} \sum_i \frac{\partial}{\partial z_{s4}} V_i, \tag{1d}$$

$$\frac{d^2}{dt^2} X = -\frac{1}{m} \sum_i \frac{\partial}{\partial X} V_i, \tag{1e}$$

$$\frac{d^2}{dt^2} Y = -\frac{1}{m} \sum_i \frac{\partial}{\partial Y} V_i, \tag{1f}$$

$$\frac{d^2}{dt^2} Z = -\frac{1}{m} \sum_i \frac{\partial}{\partial Z} V_i, \tag{1g}$$

$$\frac{d^2}{dt^2} \theta = -\frac{1}{I} \sum_i \frac{\partial}{\partial \theta} V_i + \left(\frac{d\phi}{dt}\right)^2 \sin\theta \cos\theta, \tag{1h}$$

$$\frac{d^2}{dt^2} \phi = -\frac{1}{I \sin^2\theta} \sum_i \frac{\partial}{\partial \phi} V_i - \frac{2}{\tan\theta} \left(\frac{d\theta}{dt}\right)\left(\frac{d\phi}{dt}\right), \tag{1i}$$

where $z_{s1} - z_{s4}$ represent the out-of-plane positions of the four mobile solid atoms (S1–S3 are subsurface while S4 lies on the surface); X, Y, and Z are the center-of-mass coordinates for the NO molecule; and θ and ϕ are the angles that define the projection of the internuclear axis onto the y axis and the orientation of the internuclear axis in the x–z plane, respectively (Fig. 2).[28] M, m, I, and ω are the surface atom's mass, the molecule's mass, the molecule's moment of inertia, and the vibrational frequency constant of the surface, respectively.

The total surface–molecule potential V is composed of pairwise interactions, V_i, summed over all nineteen surface atoms. The form of the pairwise interaction potential is identical to that developed by Muhlhausen, Williams, and Tully[18]:

$$V_i = A \exp(-\alpha r_{Oi}) + B\{\exp(-2\beta [r_{Oi} - r_e]) - 2\cos^2\eta_i \exp(-\beta [r_{Oi} - r_e])\}, \tag{2}$$

where

$$r_{Ni} = \{(X - x_i - R_N \sin\theta \sin\phi)^2 + (Y - y_i - R_N \cos\theta)^2 + (Z - z_i - R_N \sin\theta \cos\phi)^2\} \tag{3a}$$

$$r_{Oi} = \{(X - x_i + R_O \sin\theta \sin\phi)^2 + (Y - y_i + R_O \cos\theta)^2 + (Z - z_i + R_O \sin\theta \cos\phi)^2\}^{1/2}, \tag{3b}$$

and

$$\cos\eta_i = \frac{r_{Ni}^2 + r_{NO}^2 - r_{Oi}^2}{2 r_{Ni} r_{NO}}. \tag{3c}$$

Here, r_{Ni}, r_{Oi}, r_{NO}, R_N, and R_O correspond to the absolute magnitudes of the distances between the nitrogen atom and surface atom i, the oxygen atom and surface atom i, the NO bond distance, the nitrogen atom and the molecule's center of mass, and the oxygen atom and the molecule's center of mass, respectively. The coordinates x_i, y_i, and z_i identify the position of the surface atom i, where the origin is located at the equilibrium position of the active surface atom S4. The variable η_i defines the angle between $\mathbf{r}_{Oi}$ and $\mathbf{r}_{Ni}$. The molecule–surface potential contains an exponential repulsion term between the oxygen atom and the surface atom i, and an attractive Morse potential (with both isotropic and orientation-dependent components) between the nitrogen atom and the surface atom i. The values of the interaction potential parameters are listed in Table I. Because our model surface is unable to relax to the same extent as that of Muhlhausen *et al.*,[18] we were required to increase the B parameter by 5% in order to arrive at a similar binding energy for the atop site. Using these parameters, the calculated well depth is 105 kJ/mol and the equilibrium bond distance between the NO center of mass and the atop Pt atom is 2.3 Å. The potential energy hypersurface does not distinguish between the two fine-structure components of NO. It has a strong dependence on molecular orientation and favors linear bonding through the nitrogen atom via an atop site. The potential's predicted preference for bonding at an atop site appears to be inconsistent with recent experimental evidence which suggests that only the bridge site is occupied at low coverage.[29–32] However, these same experimental studies do find that at higher coverage the atop site is preferentially occupied. Our calculations intend to simulate rotational dynamics in the low coverage limit and may thus be biased by the

TABLE I. Interaction potential parameters.

A	61224 kJ/mol
B	96 kJ/mol
α	3.366 Å^{-1}
β	1.683 Å^{-1}
r_e	1.50 Å
$r_{Pt\text{-}Pt}$	2.75 Å
r_{NO}	1.15 Å
R_O	0.54 Å
R_N	0.61 Å
ω	3.5 ps^{-1}

model potential's inaccurate description of the surface corrugation.

All trajectories start with the NO center of mass located 6 Å from the surface.[33] The initial orientation of the molecule's internuclear axis as well as the orientation of the molecule's rotational angular momentum are randomly selected for each trajectory (see Appendix). The two-dimensional impact parameter, i.e., the point on the surface lattice where the molecule's center of mass would strike in the absence of any attractive potentials, is also stochastically varied for each trajectory. The surface temperature is established by randomly selecting initial mobile surface and subsurface positions and momenta from a Boltzmann distribution at the specified surface temperature. The inelastic scattering regime is studied using the following initial conditions: the rotational state distribution is chosen to be Boltzmann at 40 K (identical to that measured experimentally),[21] and the translational energy distribution is characterized by a supersonic expansion[34] directed at normal incidence. For the case of simulating trapping/desorption, the total angular momentum of the incident molecule is preselected so that the dynamics of a single rotational quantum state can be examined. However, the translational energy distribution is Maxwellian at the surface temperature T_s with an incident angular distribution of $\cos\theta$.

The theory of detailed balance relates desorption rotational state populations and alignment moments to trapping probabilities through the following identities:

$$P_{\text{desorption}}(J) \propto \frac{\Sigma_{i=1}^{M} P_{\text{trapping}}(N,v_i,\varphi_i)}{M} \times \exp\left(\frac{-BN(N+1)}{kT}\right), \tag{4}$$

and

$$A_{0\,\text{desorption}}^{(2)}(N) = \frac{\Sigma_{i=1}^{M} P_{\text{trapping}}(N,v_i,\varphi_i)(3\cos^2\varphi_i - 1)}{\Sigma_{i=1}^{M} P_{\text{trapping}}(N,v_i,\varphi_i)}, \tag{5}$$

where for flux-weighted probabilities

$$P_{\text{trapping}}(N,v_i,\varphi_i) = \begin{cases} 0 \text{ for trajectories which scatter,} \\ 1 \text{ for trajectories which trap,} \end{cases} \tag{6a}$$

and for number density-weighted probabilities

$$P_{\text{trapping}}(N,v_i,\varphi_i) = \begin{cases} 0 \text{ for trajectories which scatter,} \\ \dfrac{1}{v_i} \text{ for trajectories which trap.} \end{cases} \tag{6b}$$

Here, the trajectory index, i, runs from 1 to M, where M is the total number of trajectories. The initial angle between **N** and the surface normal is represented as φ_i, while v_i corresponds to the initial velocity. The equilibrium temperature of the system (both gas and surface) is T, and B is the rotational constant of the molecule.

Newton's equations of motion are integrated using standard numerical techniques (fourth-order Runga–Kutta with adaptive stepwise control).[35] The integration time step (1 fs on average) is adjusted within each trajectory calculation to minimize computation time without sacrificing accuracy. The trajectory is terminated either when the molecule scatters beyond 6 Å or when the trajectory has run for as long as 6 ps without the molecule escaping from the surface (at which time the molecule is considered trapped). Although great care has not been taken to optimize the computer code, one thousand trajectories consume four hours of CPU time on a VAX 8550 or eight hours on a MicroVAX 3600.

III. RESULTS

A. Direct and indirect inelastic scattering

Simulations of direct and indirect inelastic scattering were performed for a neat supersonic expansion of NO (9 kJ/mol translational energy) directed at normal incidence to a Pt(111) surface, at temperatures of 375 and 450 K. Those trajectories which escaped the surface were sorted according to their initial and final states. A total of 12 000 trajectories were run for each surface temperature simulation.

Figure 3 shows a Boltzmann plot of the calculated rotational excitation probabilities for inelastic scattering at 375 and 450 K. The inset presents the rotational alignment distribution (displayed by the quadrupole moment, $A_0^{(2)}$)[36] as a function of the final rotational quantum number N. The predicted rotational populations are in good agreement with the experimental curves representing the data of Jacobs *et al.*[21] The low J region of the experimental data has a significant background contribution from the incident molecular beam. This effectively dilutes the alignment measured at low J and produces anomalously high rotational populations for $J < 5.5$. The vertical dotted line marks the total energy of the incident molecular beam. If there were no transfer of energy from surface thermal motion to nuclear rotation, then rotational excitation beyond this value would be impossible. However, both experiment and theory indicate that a sizable fraction of the scattered molecules contain more rotational energy than imposed by the rigid surface limit.

Figure 4 shows the calculated correlation between final average translational energy and final rotational energy. As seen in other scattering experiments,[37–39] the translational energy is anticorrelated with rotational energy. Additionally, the average total energy of the scattered molecules rises steadily with increasing molecular rotation. It implies, however, that for most final rotational states, the average total energy of the molecules that scatter from the surface is greater than the initial beam energy of 9 kJ/mol. Thermodynamically, this is reasonable since the temperature of the surface exceeds the equivalent temperature of the beam, i.e., the temperature of the beam when its energy is equally partitioned among all of the molecule's degrees of freedom. Molecules that forfeit energy to the surface are more likely to be trapped.

To understand the role of multiple "bounces" in the scattering process, we sorted the trajectories by the number of bounces the molecule makes with the surface before escaping. A bounce is defined as a negative-to-positive change in the normal component of the molecule's linear momentum. Figure 5(a) shows the dramatic reduction of rotational alignment which accompanies additional bounces on the surface. The initial alignment produced by the first impul-

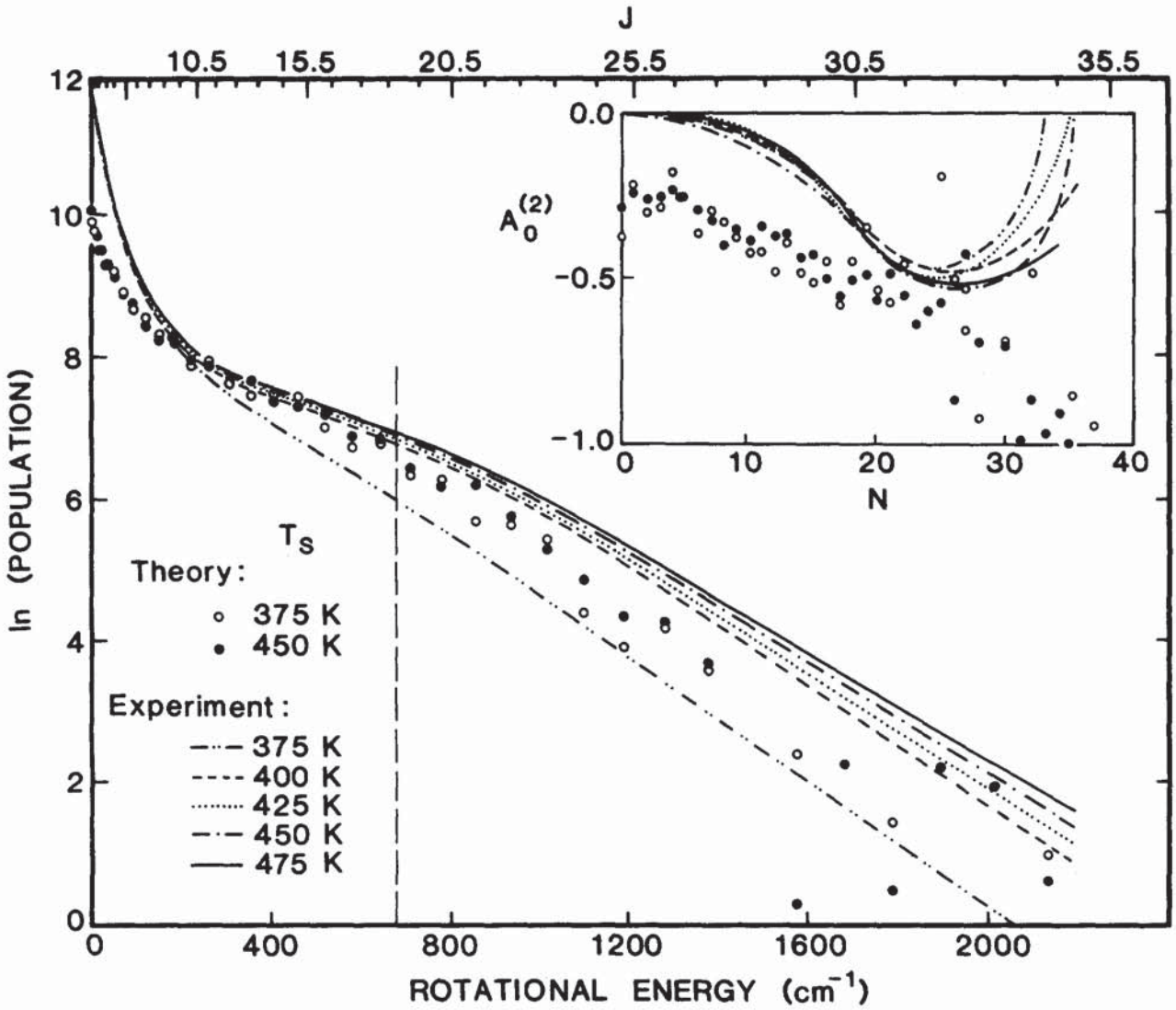

FIG. 3. Boltzmann plot of the simulated rotational distribution resulting from inelastic scattering of NO from a Pt(111) surface. The inset shows the dependence of the quadrupole alignment moment on N. (Curves correspond to experiment at the listed temperatures, (○) 375 K calculation, (●) 450 K calculation.)

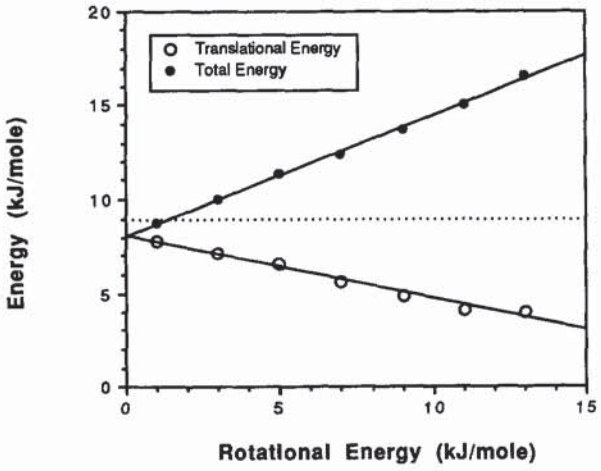

FIG. 4. The calculated variation of final translational energy and total energy with final rotational energy for NO molecules scattering from a 450 K Pt(111) surface. The dashed line represents the initial beam energy (9 kJ/mol).

sive collision with the surface becomes increasingly scrambled with each successive bounce the molecule makes with the surface. Figure 5(b) illustrates the effect of multiple bounces on the final average rotational energy of the scattered species. Trajectories which incur multiple bounces tend to have more average rotational energy with less rotational alignment. This effect might explain the drop in rotational alignment observed experimentally for the highest rotational states, i.e., indirect inelastic scattering dominates at high J.[40] Although the model's predicted alignment distribution does not exhibit the same dramatic effect, this may only indicate that the model has underestimated the fraction of multiple bounce trajectories contributing to the populations in the highest rotational states. Somewhat more surprising is the increase is translational energy with multiple bounces [Fig. 5(b)]. Examination of the trajectories reveals that the tangential component of the translational energy increases at a greater rate, with increasing bounces, than the decline in the normal component of the translational energy

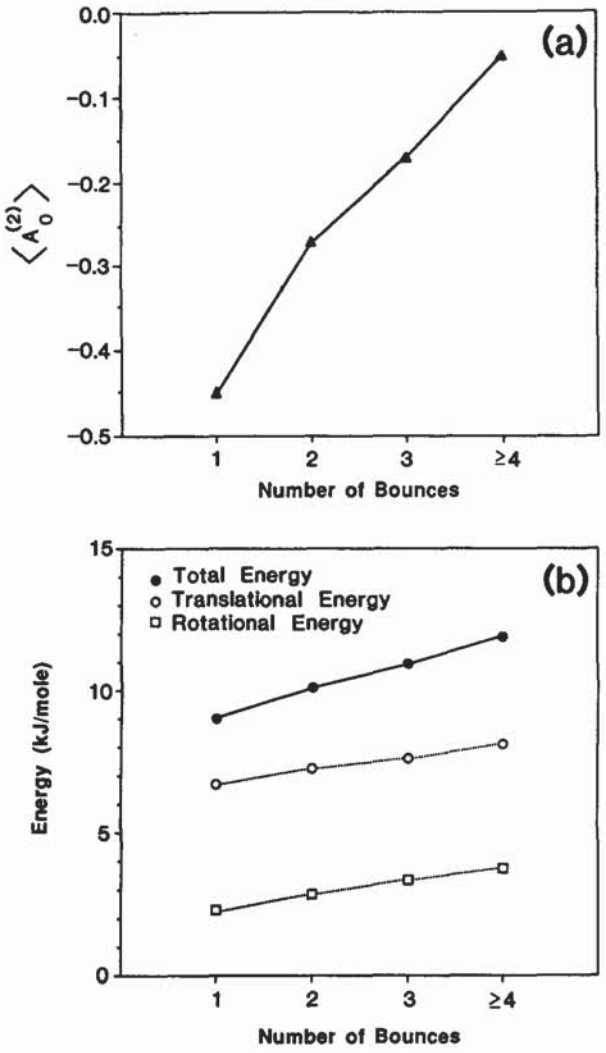

FIG. 5. Effect of multiple bounces in inelastic scattering at 450 K: (a) average rotational alignment (as measured by the quadrupole moment) and (b) final average rotational, translational, and total energies vs the number of bounces incurred prior to scattering.

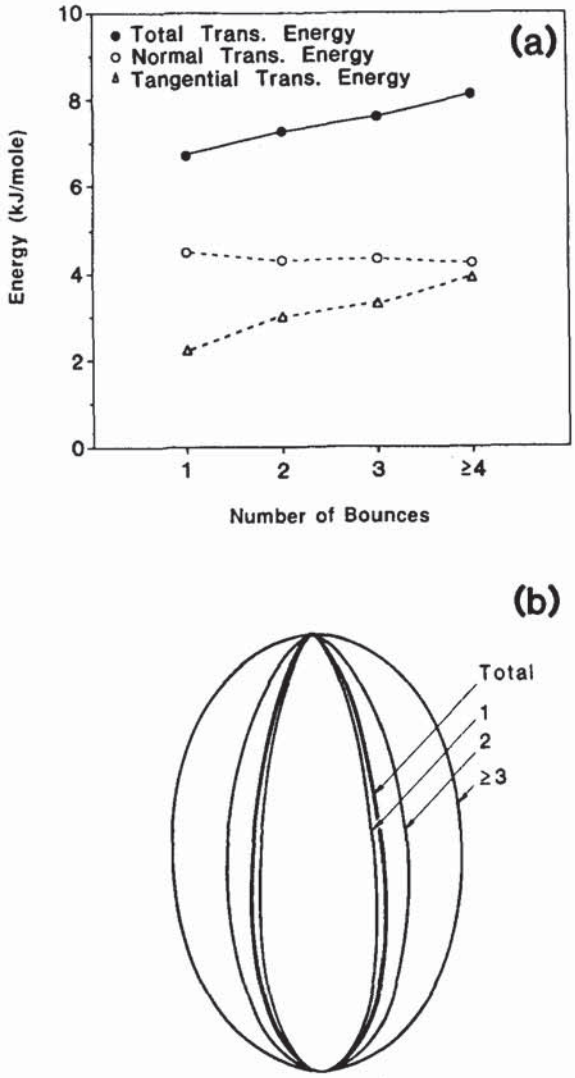

FIG. 6. Velocity distributions for scattering at 450 K: (a) tangential, normal and total translational energy components vs number of bounces and (b) velocity angular distributions in which the NO molecule makes 1, 2, or 3 (or more) bounces with the surface before escaping. The heavy line shows the total angular distribution averaged over all bounces.

[see Fig. 6(a)]. This behavior is consistent with the scattering angular distributions [see Fig. 6(b)]. The angular distribution broadens with each additional molecular bounce that occurs in the scattering process.

The increase in energy accommodation which accompanies multiple molecular bounces on the surface suggests that the trapping probability should also rise in the same fashion. Indeed, Fig. 7(a) confirms this conjecture. The escape probability, i.e., the probability that a molecule escapes the surface on its nth bounce, falls monotonically with n. A slightly different perspective [Fig. 7(b)] reveals the fraction of total scattered molecules that bounced n times before departing from the surface. After three collisions, 90% of those molecules that will scatter from the surface have already done so. For both surface temperatures, the predicted trapping probability is 0.60 ± 0.2, somewhat less than the measured values of 0.65,[41] 0.85,[42] and 0.9[43] but equivalent to the calculations of Muhlhausen *et al.*,[18] who constructed the potential used here. Hence we attribute the discrepancy to the form of the potential and not necessarily to our physical description of the surface.

The trapping probability for a trajectory also depends on its two-dimensional surface impact parameter. Figure 8 gives both a three-dimensional plot and a contour plot of the trapping probability as a function of the surface impact parameter. The highest probability for scattering occurs at the high symmetry sites—the atop and the bridge sites. The highest probability for trapping occurs when the molecule is directed toward the side of a surface atom. It is this type of collision that most effectively transfers normal momentum into tangential momentum; loss of normal momentum leads to multiple bounces, which in turn favors trapping. A similar phenomenon has been reported in calculations of the trapping dynamics of Ar on Pt(111).[16]

B. Trapping/desorption

The trajectories reported in this section are representative of an initial 550 K Maxwellian velocity distribution of NO molecules incident on the 550 K model surface. Initial rotational levels were preselected, but the spatial direction of

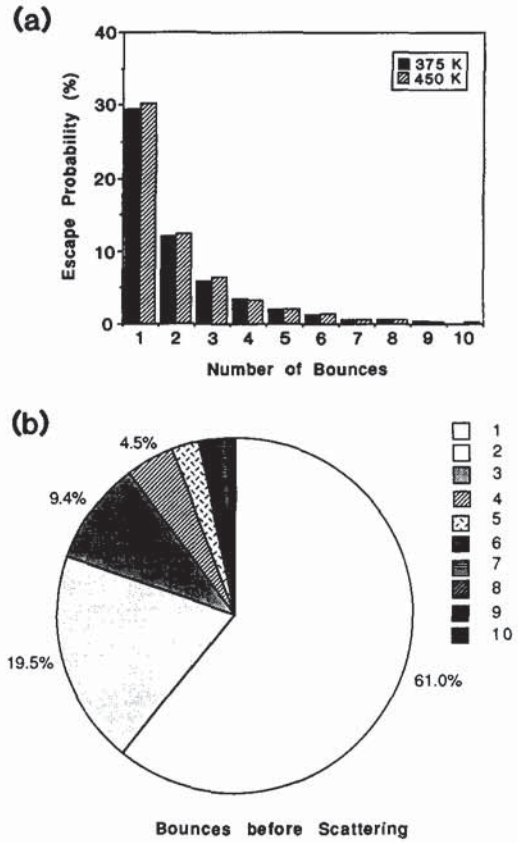

FIG. 7. The (a) probability of escape on the nth molecular bounce with the surface and (b) the fraction of the total scattered molecules that escaped on the nth bounce.

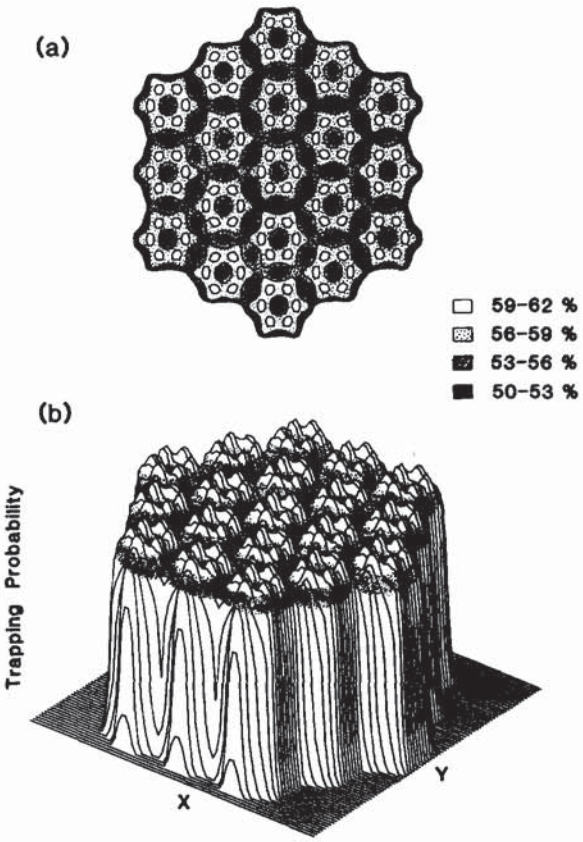

FIG. 8. Surface impact parameter dependence for trapping: (a) three-dimensional and (b) contour plots of the trapping probability for a neat supersonic beam of NO at normal incidence to a 450 K Pt(111) surface.

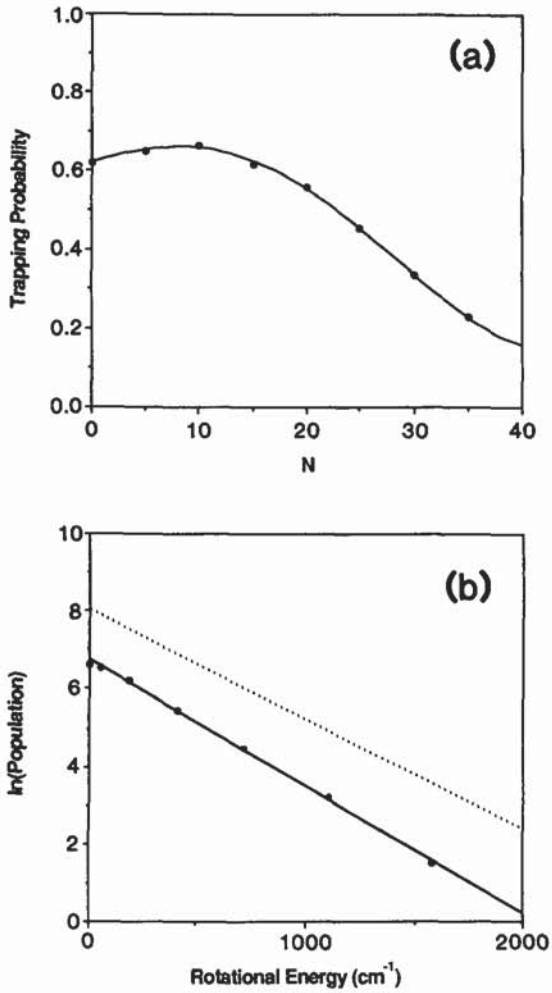

FIG. 9. (a) N-dependence of the trapping probability at 550 K and (b) Boltzmann plot of the predicted rotational distribution for desorption at 550 K.

both the rotational angular momentum and the molecular orientation were randomly selected from an isotropic distribution. Approximately 1500 trapped trajectories were computed for each initial rotational level examined. As explained in Sec. II, the calculated probability of trapping, as a function of initial conditions, is easily converted into final state distributions for the process of desorption.

The rotational state-specific trapping probability is plotted in Fig. 9(a). The overall trend indicates that a decrease in trapping accompanies an increase in rotational angular momentum. This phenomenon is indicative of an efficient transfer of rotational angular momentum to linear momentum along the surface normal, which assists the molecule in escaping the attractive potential well. In addition, one observes that the trapping probability is slightly higher for $N = 10$ than it is for $N = 0$. Analogous to gas-phase reactive collision dynamics,[44] this effect may be associated with a steric barrier to reaction for certain approach geometries. A small amount of rotational angular momentum allows the molecule to sample a variety of approach geometries which increase the probability of a reactive encounter, i.e., trapping in the present case. The J-dependent trapping probability is readily converted to a Boltzmann plot for desorption [see

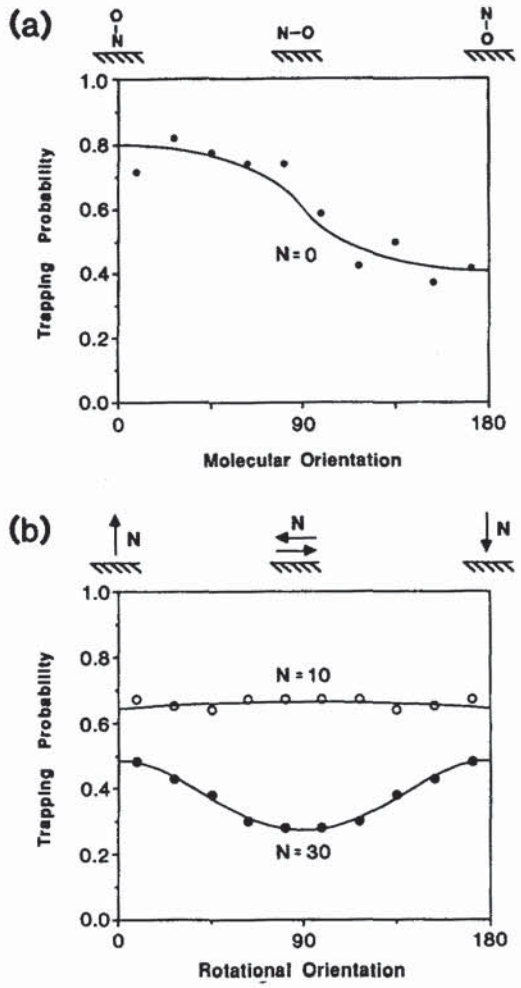

FIG. 10. Trapping probability vs (a) molecular orientation of the rotationless state, $N = 0$, and (b) rotational orientation of the $N = 10$ and $N = 30$ rotational states.

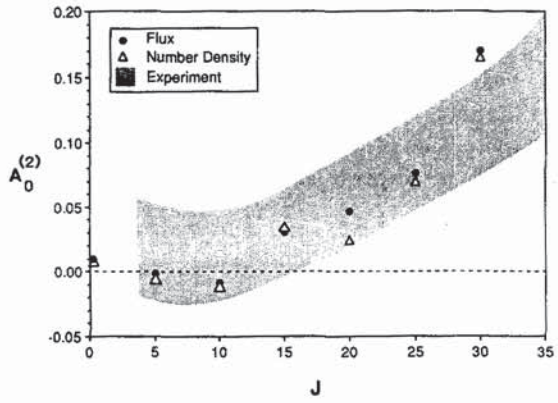

FIG. 11. Predicted alignment for NO molecules desorbing from a 550 K Pt(111) surface. The experimental data, including error bars, are represented by the shaded region while the calculated points are shown for flux-sensitive detection (●) and number-density-sensitive detection (△).

Fig. 9(b)]. The desorption rotational temperature is calculated to be 485 K, more than 60 K cooler than the surface temperature. It is interesting to compare this with the NO/Pt(111) scattering experiments of Segner *et al.*[45] which revealed a rotational temperature of 410 ± 30 K for a surface temperature of $T_s = 550$ K.

Figure 10(a) shows the dependence of the trapping probability on molecular orientation for the rotationless state, $N = 0$. It is seen that molecules that approach the surface "nitrogen end down" (nitrogen end pointing toward the surface) have twice the probability of trapping as those which approach the surface "oxygen end down".[18,46] This is a direct manifestation of the orientational anisotropy of the surface–molecule potential. On the other hand, a rotating molecule can no longer be identified as having a unique molecular orientation with respect to the surface. Instead, the direction of the angular momentum vector, **N**, is fixed (in the absence of fields) and the surface effectively samples a distribution of molecular orientations. Figure 10(b) shows the dependence of trapping on the direction of the rotational angular momentum vector for $N = 10$ and 30. The model indicates that the low N state ($J = 10$, $E_{\rm rot} = 2.4$ kJ/mol) exhibits almost no preferential alignment dependence for trapping. This is a consequence of the odd symmetry in the orientation-dependent trapping probability shown in Fig. 10(a). Regardless of the direction of **N**, an ensemble of rotating molecules will sample an equal number of molecular orientations less than 90° (favoring nitrogen end down) as those greater than 90° (favoring oxygen end down). Thus, the ensemble-averaged trapping probability will appear constant, independent of the direction of **N**. In contrast, the high N state ($N = 30$, $E_{\rm rot} = 20.5$ kJ/mol) shows a preferential alignment, which can be attributed to a dynamical effect: rotational angular momentum is more efficiently converted to linear momentum along the surface normal for molecules rotating in a plane perpendicular to the surface (**N** parallel to the surface) than for molecules rotating in a plane parallel to the surface (**N** perpendicular to the surface). It is normal linear momentum that assists the molecule in escaping the attractive well. Hence, molecules striking the surface with rotational motion resembling that of a cartwheel have a lower chance of trapping than those that approach with a helicopter motion. This latter effect only becomes important for molecules having a significant amount of rotational angular momentum. Figure 11 depicts the predicted rotational alignment of the desorbing NO molecules as a function of rotational angular momentum. The model's results are in excellent agreement with the experimental data measured by Jacobs *et al.*[24] They indicate that molecules desorbing with large amounts of rotational angular momentum will prefer to rotate in a plane parallel to the surface.

The final state velocity distribution for NO molecules desorbing from the Pt(111) surface at 550 K is predicted by the model to be 465 ± 10 K, regardless of the final rotational state. This translational temperature is lower than that measured by Guthrie *et al.*[47] (530 ± 40 K) for the same surface temperature. The predicted independence of final velocity and final rotational state has been measured for the related case of NO desorbing from an oxidized germanium surface.[37] In addition, the model predicts for NO/Pt(111) a negligible correlation between rotational alignment and velocity. Taken together, these two predictions suggest that the translational and rotational degrees of freedom separate to

good approximation in describing trapping followed by desorption. However, the model does imply that the magnitude of rotational alignment associated with desorption will decrease for increasing surface temperature. Specifically, the quadrupole moment for $N = 30$ is calculated to be 0.21, 0.17, and 0.14 for surface temperatures of 350, 550, and 750 K, respectively.

IV. DISCUSSION

A simple classical trajectory method has been put forth to model the dynamics of inelastic scattering and trapping/desorption. The model is appealing in that the comprehensive information revealed by a trajectory analysis is realized with the use of conventional computational facilities. As a first test, the model was applied to the NO/Pt(111) system. The quality of agreement between experiment and theory surpassed our expectations. Although the results of the model are consistent with a collection of experimental measurements, we can only speculate on whether the model's premise is accurate or fortuitous.

The model included limited surface motion. Specifically, the surface atom closest to the molecule translated only in the direction of the surface normal. The mobile platinum atoms were harmonically coupled and described with a single spring constant. However, variation of the spring constant by a factor of two had little effect on the resulting dynamics. Additionally, we sorted trajectories according to their two-dimensional surface impact parameter. Trajectories that were directed toward the atop site yielded similar final state distributions as those trajectories that were directed towards the bridge site.[48] We conclude that while surface motion is essential for an accurate description of this system, the details of that motion play a secondary role in modeling the rotational dynamics. The same conclusion has been reached previously by Tully[17] based on his complete GLE studies.

We utilized the empirical NO/Pt(111) potential developed by Muhlhausen, Williams and Tully.[18] Great care on their part went into determining the parametrization and general features of this potential hypersurface. Although we did not vary the surface–molecule potential, it appears that the potential's large anisotropy with respect to molecular orientation plays a major role in the transference of initial translational energy and surface vibrational energy into final rotational energy. The corrugation of the surface, as manifested by the surface–molecule potential, contributes to the imperfect degree of rotational alignment calculated in the regime of direct and indirect inelastic scattering. This is because a corrugated surface exerts forces, on the scattering molecule, that do not necessarily lie along the surface normal. These forces may lead to rotational excitation outside of the limiting case of pure cartwheel motion.

The predictions of the model, along with a variety of experimental observations, help to construct a dynamical picture of the interactions of nitric oxide with a clean Pt(111) surface. An incident nitric oxide molecule begins to sense the attractive part of the potential approximately 5 Å from the surface. As the molecule accelerates toward the surface, it experiences a torque which attempts to swing the nitrogen-end of the molecule toward the surface. At the deepest part of the potential (approximately 2.3 Å from the surface) the system has gained as much as 105 kJ/mol of additional kinetic energy, in the form of translation, rotation and surface vibration.

The repulsive part of the potential serves to transfer energy efficiently between the different degrees of freedom in the system. As seen in the simple case of scattering ellipsoids off of hard cubes,[10] translational $\Leftrightarrow$ rotational energy transfer can be very strong for certain molecular orientations. More specifically, it has been shown that scattering of a rotationally cold, translationally hot beam of molecules from a surface produces a distribution of rotationally excited states that are highly aligned (with a propensity toward cartwheel motion).[39,49–51] Of course, this rotational excitation occurs at the expense of translational energy. Note that the converse must also be true, i.e., a rotationally excited beam of molecules (favoring cartwheel motion) will gain translational energy at the cost of rotational energy upon scattering from a surface. If during the collision the surface atom closest to the NO molecule is moving into the bulk, then, in general, the molecule will lose energy and momentum to the surface. If, however, the same surface atom is translating out of the bulk, the NO molecule will gain translational and/or rotational energy. The surface corrugation assists in converting linear momentum along the surface normal into tangential momentum for those trajectories that strike the surface on the side of an atop site.

Together, these effects prepare the molecule for its attempt to escape the attractive potential well of the surface. It is only linear momentum along the surface normal and nuclear rotation[52] that are capable of being converted into the potential energy required to surmount the barrier to desorption. If these two forms of energy are deficient, then the molecule is forced to collide with the surface once again. Each additional collision with the surface increases the chance of trapping. On average, those molecules that are able to escape on the first few bounces have gained energy from the surface. As shown, the effect of increased bounces on trajectories that scatter is a decrease in rotational alignment, an increase in rotational energy, a decrease in normal translational energy and a broadening of the scattered angular distribution.

The process of trapping is most dramatically inhibited in cases where (i) the incident molecule is highly rotationally excited (This is especially true if the rotational motion is aligned similar to that of a cartwheel.), (ii) a slowly rotating or nonrotating molecule strikes the surface oxygen end first (this samples a shallower potential well and it leads preferentially to cartwheel motion that facilitates escape), or (iii) the molecule is directed toward an atop site or bridge site on the surface (here translational energy along the surface normal is not efficiently converted to tangential translational energy).

The process of desorption occurs over a much longer timescale. However, the desorption dynamics are determined by the last few encounters the molecule makes with the surface. We speculate that the molecule undergoes hindered rotation on the surface prior to desorption. On the

surface, rotation resembling that of a cartwheel is more strongly hindered than that resembling a helicopter. Therefore, the molecule is most likely librating with the oxygen end precessing around the nitrogen end, which is pinned to the surface by the strong chemisorption bond. Breakage of the Pt–NO bond in this transition state preferentially leads to desorbates whose rotational motion resembles that of a helicopter.[53]

It is difficult to comment on the generality of these conjectures. Further experiments and calculations on various other molecule–surface systems are certainly required. However, we feel that many heteronuclear diatomic molecules will exhibit similar dynamics for interactions with a variety of metal surfaces for which the interaction potential is strong and anisotropic.

ACKNOWLEDGMENTS

This work was supported by the Office of Naval Research (N00014-87-K-00265). D. C. J. wishes to thank Kurt W. Kolasinski and Stacey F. Shane for helpful discussions.

APPENDIX

This appendix provides a few of the pertinent equations required to perform similar trajectory calculations. We give a brief overview of the stochastic selection of initial conditions and the reduction of final state coordinates and momenta into a more useful form.

The initial coordinates and momenta are stochastically selected at the beginning of each trajectory. The following equations utilize a uniform deviate, x_i, which is a random number between 0 and 1. The computer selects a uniform deviate for each variable i within each trajectory.

The choice of surface impact parameter begins with

$$X = 1.3 r_{\mathrm{Pt\text{-}Pt}} [x_1 - \tfrac{1}{2}], \tag{A1a}$$

$$Y = r_{\mathrm{Pt\text{-}Pt}} [x_2 - \tfrac{1}{2}], \tag{A1b}$$

where $r_{\mathrm{Pt\text{-}Pt}}$ is the platinum–platinum atom equilibrium separation on the surface. After X and Y are selected, they are tested to insure that they lie within the shaded region of Fig. 1. If they do not, then uniform deviates are rechosen until this condition is met.

The positions and momenta of the mobile surface and subsurface atoms are selected individually:

$$z_{Si} = z_{S(i-1)} + \frac{1}{\omega}\sqrt{-2\frac{kT}{M}\ln x_3}\cos[2\pi x_4], \tag{A2a}$$

$$\frac{d}{dt} z_{Si} = \sqrt{-2\frac{kT}{M}\ln x_3}\sin[2\pi x_4], \tag{A2b}$$

where $i = 1$–3 for the subsurface atoms and $i = 4$ for the surface atom. Although the calculation of the position and the momentum for a single atom utilizes the same two deviates (x_3 and x_4), each atom receives a fresh pair of uniform deviates during each trajectory initialization.

For the case of inelastic scattering, the selection of the rotational state, N, in the incident molecular beam is a two-step process. First, the probability factors, $X(N')$, are calculated:

$$X(N') = \sum_{N=0}^{N'} (2N+1)\exp\left(\frac{-BN(N+1)}{kT}\right) \Bigg/ \sum_{N=0}^{\infty} (2N+1)\exp\left(\frac{-BN(N+1)}{kT}\right). \tag{A3}$$

Next, a uniform deviate, x_5, is used to find the value of one N' that satisfies the following inequality:

$$X(N'-1) < x_5 \leqslant X(N'). \tag{A4}$$

The initial state N is preselected for the case of trapping/desorption simulations.

In both modeling regimes, selection of the direction of **N** as well as the orientation of the internuclear axis requires the use of three random Euler angles:

$$\alpha = \cos^{-1}(2x_6 - 1), \tag{A5a}$$

$$\beta = 2\pi x_7, \tag{A5b}$$

$$\gamma = 2\pi x_8, \tag{A5c}$$

which in turn uniquely define the spherical angles and angular velocities:

$$\theta = \cos^{-1}\{\cos\beta\cos\gamma - \cos\alpha\sin\beta\sin\gamma\}, \tag{A6a}$$

$$\phi = \tan^{-1}\left\{\frac{-\sin\beta\cos\gamma - \cos\alpha\cos\beta\sin\gamma}{\sin\alpha\sin\gamma}\right\}, \tag{A6b}$$

$$\frac{d}{dt}\phi = \sqrt{\frac{2BN(N+1)}{I}}\left[\frac{\sin\alpha\sin\beta}{\sin^2\theta}\right], \tag{A6c}$$

and

$$\frac{d}{dt}\theta = \sqrt{\frac{2BN(N+1)}{I} - \left[\sin\theta\left(\frac{d\phi}{dt}\right)\right]^2}. \tag{A6d}$$

The beam velocity for the inelastic scattering simulations is directed along the surface normal:

$$\frac{d}{dt} Z = -\sqrt{\frac{2E}{m}} + \sqrt{-2\frac{kT_{\mathrm{beam}}}{m}\ln x_9}\sin(2\pi x_{10}). \tag{A7}$$

Here, E is the translational energy and T_{beam} is the internal translational temperature of the supersonic beam. Modeling of trapping/desorption utilizes a spatially isotropic Maxwellian distribution of incident velocities:

$$\frac{d}{dt} X = \sqrt{-2\frac{kT}{m}\ln x_{11}}\sin(2\pi x_{12}), \tag{A8a}$$

$$\frac{d}{dt} Y = \sqrt{-2\frac{kT}{m}\ln x_{13}}\sin(2\pi x_{14}), \tag{A8b}$$

and

$$\frac{d}{dt} Z = -\sqrt{-2\frac{kT}{m}\ln x_{15}}\sin(\pi x_{16}). \tag{A8c}$$

However, this incident distribution must be weighted by the velocity's projection onto the surface normal. This insures that we are properly treating the incident velocity distribu-

tion as a flux onto the surface. Hence, if

$$x_{17} \geqslant -\left(\frac{d}{dt}Z\right) \Big/ \sqrt{\left(\frac{d}{dt}X\right)^2 + \left(\frac{d}{dt}Y\right)^2 + \left(\frac{d}{dt}Z\right)^2}\,, \tag{A9}$$

then Eqs. (A8a)–(A8c) must be reevaluated with new uniform deviates.

Equations (A1)–(A9) provide a complete stochastic set of initial conditions for individual trajectories within a series. It is useful to be able to determine relevant energies and vector directions for the system at any point during the trajectory. The rotational energy, semi-classical rotational quantum number N, and the projection of $\mathbf{N}$ on the surface normal (as defined by φ) are computed as follows:

$$E_{\rm rot} = \frac{1}{2} I \left\{ \sin^2\theta \left(\frac{d\phi}{dt}\right)^2 + \left(\frac{d\theta}{dt}\right)^2 \right\}, \tag{A10a}$$

$$N = \frac{1}{2}\left\{ -1 + \sqrt{1 + 4\frac{E_{\rm rot}}{B}} \right\}, \tag{A10b}$$

and

$$\varphi = \cos^{-1}\left\{ \frac{-\sin\phi(d\theta/dt) - \cos\theta\sin\theta\cos\phi(d\phi/dt)}{\sqrt{\sin^2\theta(d\phi/dt)^2 + (d\theta/dt)^2}} \right\}. \tag{A10c}$$

The energy of the mobile surface atoms is calculated through the following summation:

$$E_{\rm surf} = \sum_{i=1}^{4} \frac{1}{2} M \left\{ \left(\frac{dz_{Si}}{dt}\right)^2 + \omega^2 (z_{Si} - z_{S(i-1)})^2 \right\}. \tag{A11}$$

The translational energy of the molecule and ϑ, the angle between the velocity vector and the surface normal, are computed from the first derivatives of the center-of-mass coordinates:

$$E_{\rm trans} = \frac{1}{2} m \left\{ \left(\frac{d}{dt}X\right)^2 + \left(\frac{d}{dt}Y\right)^2 + \left(\frac{d}{dt}Z\right)^2 \right\}, \tag{A12a}$$

and

$$\vartheta_{\rm vel} = \cos^{-1}\left[\left(\frac{d}{dt}Z\right) \Big/ \sqrt{\left(\frac{d}{dt}X\right)^2 + \left(\frac{d}{dt}Y\right)^2 + \left(\frac{d}{dt}Z\right)^2} \right]. \tag{A12b}$$

Following each trajectory, we store the "vital statistics" (both initial and final conditions) in a file. At a later point, this information is sorted according to a variety of criteria, and a detailed analysis is performed.

[1] F. O. Goodman and H. Y. Wachman, *Dynamics of Gas–Surface Scattering* (Academic, New York, 1976) and references therein.
[2] H. Voges and R. Schinke, Chem. Phys. Lett. **100**, 245 (1983).
[3] R. I. Masel, R. P. Merrill, and W. H. Miller, Surf. Sci. **46**, 681 (1974).
[4] W. Steele, Surf. Sci. **38**, 1 (1973).
[5] J. C. Polanyi and R. J. Wolf, J. Chem. Phys. **82**, 1555 (1985).
[6] C. Kuan, H. Mayne, and R. J. Wolf, Chem. Phys. Lett. **133**, 415 (1987).
[7] R. M. Logan and R. Stickney, J. Chem. Phys. **44**, 195 (1966).
[8] J. D. Doll, J. Chem. Phys. **66**, 5709 (1977).
[9] E. Grimmelmann, J. C. Tully, and M. Cardillo, J. Chem. Phys. **72**, 1039 (1980).
[10] J. E. Hurst, Jr., G. D. Kubiak, and R. N. Zare, Chem. Phys. Lett. **93**, 235 (1982).
[11] R. W. Zwanzig, J. Chem. Phys. **32**, 1173 (1960).
[12] H. K. Shin, Chem. Phys. Lett. **133**, 129 (1987).
[13] S. Adelman and J. Doll, J. Chem. Phys. **61**, 4242 (1974).
[14] S. Adelman and J. Doll, J. Chem. Phys. **64**, 2375 (1976).
[15] S. Adelman, J. Chem. Phys. **71**, 4471 (1979).
[16] J. C. Tully, Acc. Chem. Res. **14**, 188 (1981).
[17] J. C. Tully, J. Chem. Phys. **73**, 1975 (1980).
[18] C. W. Muhlhausen, L. R. Williams, and J. C. Tully, J. Chem. Phys. **83**, 2594 (1985).
[19] For example, see P. Roubin, D. Chandesris, G. Rossi, J. Lecante, M. C. Desjonqueres, and G. Treglia, Phys. Rev. Lett. **56**, 1272 (1986).
[20] For example, see G. Brusdeylins, R. Rechsteiner, J. G. Skofronick, J. P. Toennies, G. Benedek, and L. Miglio, Phys. Rev. Lett. **54**, 466 (1985).
[21] D. C. Jacobs, K. W. Kolasinski, S. F. Shane, and R. N. Zare, J. Chem. Phys. **91**, 3182, 1989.
[22] E. K. Grimmelmann, J. C. Tully, and E. Helfand, J. Chem. Phys. **74**, 5300 (1981).
[23] J. C. Tully, Surf. Sci. **111**, 461 (1981).
[24] D. C. Jacobs, K. W. Kolasinski, R. J. Madix, and R. N. Zare, J. Chem. Phys. **87**, 38 (1987).
[25] The surface harmonic frequency constant, ω, is approximately given by $0.75k\Theta_b/h$, where Θ_b is the bulk Debye temperature.
[26] In actuality, the coordinates remain unchanged during a switch of active zones. Instead, the molecule's linear and angular momenta are reflected through the active zone boundary plane through which the molecule is passing at the time of the switch. Due to symmetry, this is equivalent to having the molecule reenter the active zone from the opposite side.
[27] M. Asscher, W. L. Guthrie, T.-H. Lin, and G. A. Somorjai, J. Chem. Phys. **78**, 6992 (1983).
[28] Equation (1i) has a singularity at the point where $\sin\theta$ equals zero. Numerical integration near this point is difficult and the integration time step must be reduced dramatically. Definition of the angle θ relative to the y axis rather the z axis moves the location of the pole to a region which is sampled less frequently, given the form of the potential and the propensity for cartwheel motion. Consequently, this choice speeds up the computations by a significant factor.
[29] H. Ibach and S. Lehwald, Surf. Sci. **76**, 1 (1978).
[30] J. L. Gland and B. A. Sexton, Surf. Sci. **94**, 355 (1980).
[31] B. E. Hayden, Surf. Sci. **131**, 419 (1983).
[32] M. Kiskonava, G. Pirug, and H. P. Bonzel, Surf. Sci. **136**, 285 (1984).
[33] The depth of the molecule–surface potential at 6 Å is $<1\%$ of the well depth. Trajectories run with an 8 Å start position yielded similar results.
[34] J. Serri, M. Cardillo, and G. Becker, J. Chem. Phys. **77**, 2175 (1982) measured a translational energy of 9 kJ/mol for a neat beam of NO under similar expansion conditions. We assumed that the thermal speed of velocities within the beam could be estimated by a temperature of 30 K, or 75% of the measured rotational temperature.
[35] W. H. Press, B. P. Flannery, S. A. Teukolsky, and W. T. Vetterling, *Numerical Recipes* (Cambridge University, Cambridge, 1986), p. 554.
[36] D. C. Jacobs and R. N. Zare, J. Chem. Phys. **85**, 5457 (1986).
[37] A. Mödl, T. Grisch, F. Budde, T. Chuang, and G. Ertl, Phys. Rev. Lett. **57**, 384 (1986).
[38] C. Rettner, J. Kimman, F. Fabre, D. Auerbach, J. Barker, and J. Tully, J. Vac. Sci. Technol. A **5**, 508 (1987).
[39] G. O. Sitz, A. C. Kummel, and R. N. Zare, J. Chem. Phys. **89**, 2558 (1988).
[40] The quantum number J refers to the total angular momentum in NO. It includes nuclear rotation, orbital angular momentum and electronic spin. J, rather than N, is the good quantum number for NO. However, since the model only includes nuclear rotation, the theoretical data uses the quantum number N.
[41] T.-H. Lin and G. Somorjai, Surf. Sci. **107**, 573 (1981).
[42] C. Campbell, G. Ertl, and J. Segner, Surf. Sci. **115**, 309 (1982).
[43] J. Serri, M. Cardillo, and G. Becker, J. Chem. Phys. **77**, 2175 (1982).
[44] M. Broida, M. Tamir, and A. Persky, Chem. Phys. **110**, 83 (1986), and references therein.
[45] J. Segner, H. Robata, W. Vielhaber, G. Ertl, F. Frenkel, J. Häger, W. Krieger, and H. Walther, Surf. Sci. **131**, 273 (1983).
[46] A. Held and P. Yodzis, General Relatively Gravitation **13**, 873 (1981).

[47]W. Guthrie, T. Lin, S. Ceyer, and G. Somorjai, J. Chem. Phys. **76**, 6398 (1982).
[48]In the model, a molecule which strikes a bridge site can only sense motion in one of the two surface atoms. This artifact of the model could potentially bias the dynamics of this subset of trajectories.
[49]A. Luntz, A. Kleyn, and D. Auerbach, Phys. Rev. B **25**, 4273 (1982).
[50]A. Kleyn, A. Luntz, and D. Auerbach, Surf. Sci. **117**, 33 (1982).
[51]A. Kleyn, A. Luntz, and D. Auerbach, Surf. Sci. **152/153**, 99 (1985).
[52]For this anisotropic molecule–surface potential, rotation of the nitrogen atom away from the surface converts considerable kinetic energy into potential energy.
[53]Indeed, this picture suggests that measurement of the orientation of the rotationless state ($N = 0$, $J = 1/2$ or $3/2$ for the two spin–orbit states) will reveal that the nitrogen atom preferentially points toward the surface during desorption. Experimentally, the effect should be more substantial for the case of $J = 3/2$, because of increased interference from hyperfine depolarization in the former case.